Electronic Supplementary Material (ESI) for Journal of Materials Chemistry B.
This journal is © The Royal Society of Chemistry 2018

Intracellular delivery of peptide drugs using viral nanoparticles of bacteriophage P22: covalent loading and cleavable release

Jigang Wang,[ab] Ti Fang,[a] Ming Li,[ab] Wenjing Zhang,[ab] Zhi-Ping Zhang,[a] Xian-En Zhang,*[c] Feng Li*[a]

[a]State Key Laboratory of Virology, Wuhan Institute of Virology, Chinese Academy of Sciences, Wuhan, 430071, China. Email: fli@wh.iov.cn

[b]University of Chinese Academy of Sciences, Beijing, 100049, China

[c]National Laboratory of Biomacromolecules, CAS Center for Excellence in Biomacromolecules, Institute of Biophysics, Chinese Academy of Sciences, Beijing, 100101, China. Email: zhangxe@ibp.ac.cn

Supplementary Methods.

S1. Protein identification using LC-MS/MS.

The band of interest in SDS-PAGE was excised and was subject to in-gel digestion with 0.025 μg/μL trypsin. The purified VNP samples were digested with 0.025 μg/μL trypsin. The resulting peptides were analyzed on a hybrid quadrupole-TOF LC/MS/MS mass spectrometer (TripleTOF 5600+, AB Sciex) equipped with a nanospray source. Raw data were analyzed with the ProteinPilot Software. Data were searched against the UniProt *E. coli* and *Salmonella* phage P22 database supplemented with the complete amino acid sequences of P22-P_2, EGFP-SP and -30GFP-SP. For estimation of relative abundance of P22-P_2 and SP or SP fusion proteins in the same sample, a spectral sampling method was used.[1]

S2. Dynamic light scattering measurement of VNPs.

VNP samples at a concentration of 0.5 mg/mL were filtered by centrifugation at 5, 000 rpm in a 0.22 μm Ultrafree centrifugal filter unit (Millipore) and then measured on a zetasizer Nano ZS (Malvern) at room temperature (25 °C).

Supplementary Figures

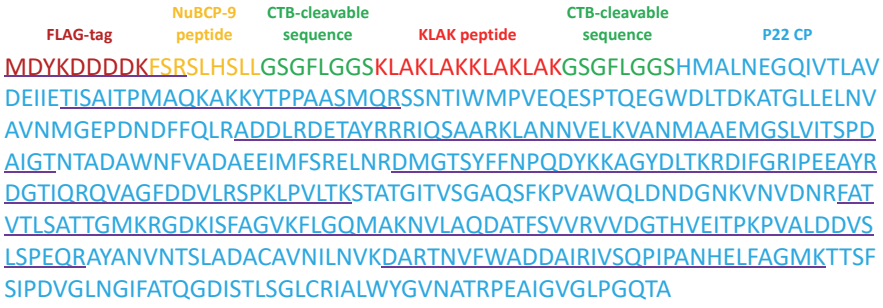

Fig. S1. Analysis of the band (a0) having a similar molecular weight of P22 CP in the SP/P22-P_2 lane in Fig. 2A. The band was excised and analyzed using in-gel trypsin digestion and LC-MS/MS, resulting in the peptide coverage map against P22-P_2. The figure shows the complete amino acid sequence of P22-P_2. The underlined amino acid sequences indicate the detected fragments. The result supports that band a0 is probably the products of nonspecific degradation of the P22-P_2 fusion protein, rather than products of protein lysis specifically at the CTB-cleavable sites.

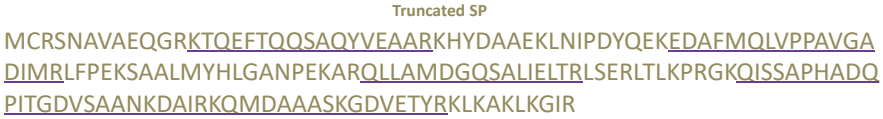

Fig. S2. Detection of the truncated SP in the purified SP/P22-P_2 VNPs. The sample was analyzed using trypsin digestion and LC-MS/MS, resulting in the peptide coverage map against the truncated SP. The figure shows the complete amino acid sequence of truncated SP. The underlined sequences indicate detected SP fragments.

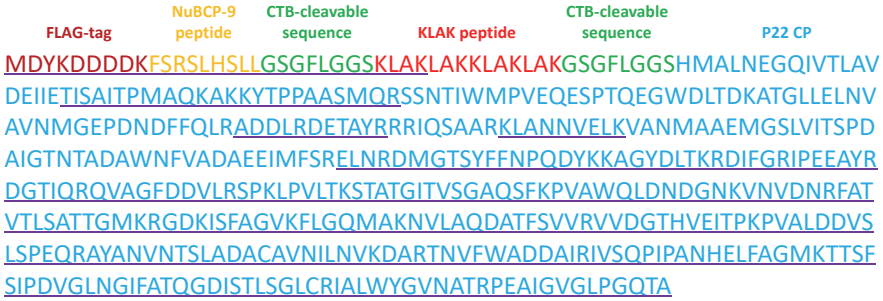

Fig. S3. Analysis of band a1 in Fig. 3A. The band was excised and analyzed using in-gel trypsin digestion and LC-MS/MS, resulting in the peptide coverage map against P22-P_2. The figure shows the complete amino acid sequence of P22-P_2. The underlined sequences indicate the detected fragments. The result supports that band a1 is probably the products of nonspecific degradation of the P22-P_2 fusion protein, rather than products of protein lysis specifically at the CTB-cleavable sites.

Fig. S4. Analysis of band b1 in Fig. 3A. The band was excised and analyzed using in-gel trypsin digestion and LC-MS/MS, resulting in the peptide coverage maps against P22-P_2 (upper) and EGFP-SP (lower). The figure shows the complete amino acid sequences of P22-P_2 (upper) and EGFP-SP (lower). The underlined sequences indicate the detected fragments. The result shows that band b1 also contains partially degraded P22-P_2 in addition to EGFP-SP.

FLAG-tag NuBCP-9 peptide CTB-cleavable sequence KLAK peptide CTB-cleavable sequence P22 CP

MDYKDDDDKFSRSLHSLLGSGFLGGSKLAKLAKKLAKLAKGSGFLGGSHMALNEGQIVTLAV
DEIIETISAITPMAQKAKKYTPPAASMQRSSNTIWMPVEQESPTQEGWDLTDKATGLLELNV
AVNMGEPDNDFFQLRADDLRDETAYRRRIQSAARKLANNVELKVANMAAEMGSLVITSPD
AIGTNTADAWNFVADAEEIMFSRELNRDMGTSYFFNPQDYKKAGYDLTKRDIFGRIPEEAYR
DGTIQRQVAGFDDVLRSPKLPVLTKSTATGITVSGAQSFKPVAWQLDNDGNKVNVDNRFAT
VTLSATTGMKRGDKISFAGVKFLGQMAKNVLAQDATFSVVRVVDGTHVEITPKPVALDDVS
LSPEQRAYANVNTSLADACAVNILNVKDARTNVFWADDAIRIVSQPIPANHELFAGMKTTSF
SIPDVGLNGIFATQGDISTLSGLCRIALWYGVNATRPEAIGVGLPGQTA

-30GFP-SP

MGASKGEELFDGVVPILVELDGDVNGHEFSVRGEGEGDATEGELTLKFICTTGELPVPWPTL
VTTLTYGVQCFSDYPDHMDQHDFFKSAMPEGYVQERTISFKDDGTYKTRAEVKFEGDTLVN
RIELKGIDFKEDGNILGHKLEYNFNSHDVYITADKQENGIKAEFEIRHNVEDGSVQLADHYQQ
NTPIGDGPVLLPDDHYLSTESALSKDPNEDRDHMVLLEFVTAAGIDHGMDELYKGGGGSGR
SNAVAEQGRKTQEFTQQSAQYVEAARKHYDAAEKLNIPDYQEKEDAFMQLVPPAVGADIM
RLFPEKSAALMYHLGANPEKARQLLAMDGQSALIELTRLSERLTLKPRGKQISSAPHADQPIT
GDVSAANKDAIRKQMDAAASKGDVETYRKLKAKLKGIR

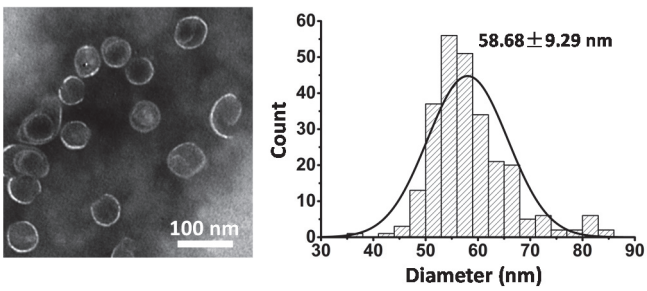

Fig. S5. Analysis of band a2 in Fig. 3A. The band was excised and analyzed using in-gel trypsin digestion and LC-MS/MS, resulting in the peptide coverage maps against P22-P_2. The figure shows the complete amino acid sequences of P22-P_2. The underlined sequences indicate the detected fragments. The result supports that band a2 is probably the products of nonspecific degradation of the P22-P_2 fusion protein, rather than products of protein lysis specifically at the CTB-cleavable sites.

Fig. S6. Analysis of band b2 in Fig. 3A. The band was excised and analyzed using in-gel trypsin digestion and LC-MS/MS, resulting in the peptide coverage maps against P22-P_2 (upper) and -30GFP-SP (lower). The figure shows the complete amino acid sequences of P22-P_2 (upper) and -30GFP-SP (lower). The underlined sequences indicate the detected fragments. The result shows that band b2 also contains partially degraded P22-P_2 in addition to -30GFP-SP.

Fig. S7. TEM images of P22 VNPs with corresponding size distribution obtained from *ca*. 250 particles. The value on the distribution graph is the average diameter of VNPs shown as mean ± SD. Scale bar: 100 nm.

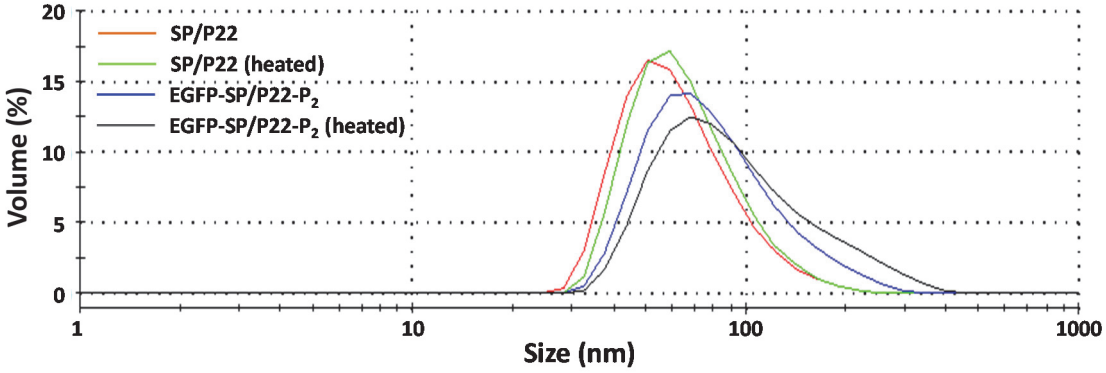

Fig. S8. DLS measurement of SP/P22 and EGFP-SP/P22-P_2 VNPs before and heat treatment.

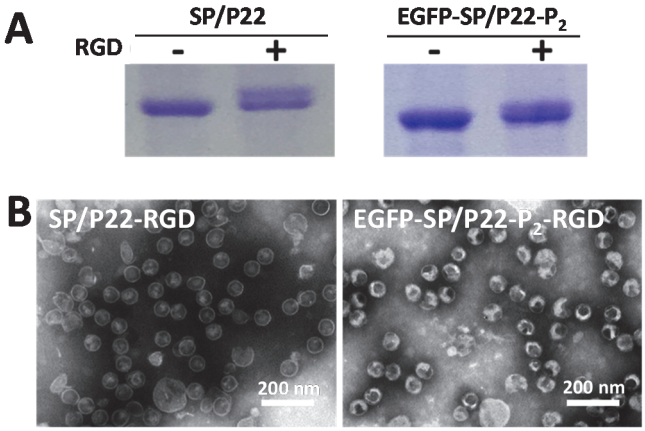

Fig. S9. Modification of P22 VNPs with synthetic RGD peptide. (A) SDS-PAGE, showing minor increases of molecular weight of CP and CP-cargo fusion protein. (B) TEM images of RGD-modified P22 VNPs. Scale bars: 200 nm.

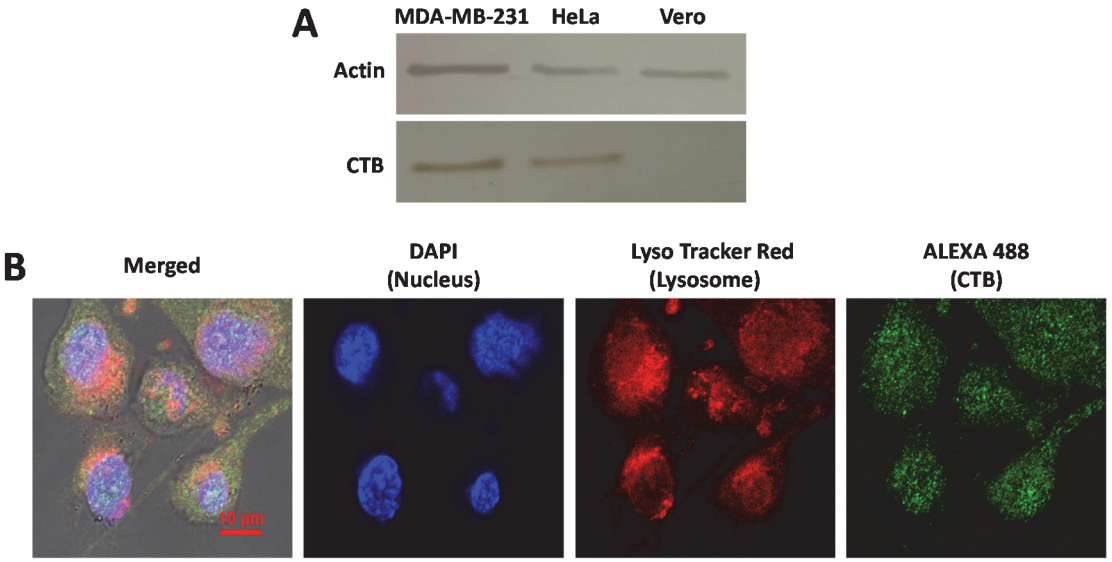

Fig. S10. Up-expression of CTB in tumor cells and its subcellular distribution. (A) Western blotting of lysates of different cell lines using an anti-CTB antibody. CTB expression levels varied in different cell lines. Three cell lines, a human breast cancer cell line (MDA-MB-231), a cervical cancer cell line (HeLa) and an African Green Monkey Kidney cell line (Vero) were compared. CTB was detected in MDA-MB-231 cells and HeLa cells but not in Vero cells. (B)

Partial colocalization of CTB (green) with lysosome (red) in MDA-MB-231 cells, revealed by immunofluorescence microscopy using an anti-CTB antibody. Scale bar: 10 μm.

Reference:

1. H. Liu, R. G. Sadygov and J. R. Yates, 3rd, *Anal. Chem.*, 2004, **76**, 4193-4201.